Comparative In Vivo Evaluation of Technetium and Iodine Labels on an Anti-HER2 Affibody for Single-Photon Imaging of HER2 Expression in Tumors

Anna Orlova, PhD[1,2]; Fredrik Y. Nilsson, PhD[1,2]; Maria Wikman, PhD[3]; Charles Widström, MSc[4]; Stefan Ståhl, PhD[3]; Jörgen Carlsson, PhD[2]; and Vladimir Tolmachev, PhD[1,2]

[1]Affibody AB, Bromma, Sweden; [2]Unit of Biomedical Radiation Sciences, Department of Oncology, Radiology, and Clinical Immunology, Rudbeck Laboratory, Uppsala University, Uppsala, Sweden; [3]Department of Biotechnology, AlbaNova University Center, Royal Institute of Technology (KTH), Stockholm, Sweden; and [4]Section of Hospital Physics, Department of Oncology, Uppsala University Hospital, Uppsala, Sweden

In vivo diagnosis with cancer-specific targeting agents that have optimal characteristics for imaging is an important development in treatment planning for cancer patients. Overexpression of the HER2 antigen is high in several types of carcinomas and has predictive and prognostic value, especially for breast cancer. A new type of targeting agent, the Affibody molecule, was described recently. An Affibody dimer, His_6-$(Z_{HER2:4})_2$ (15.4 kDa), binds to HER2 with an affinity of 3 nmol/L and might be used for the imaging of HER2 expression. The use of ^{99m}Tc might improve the availability of the labeled conjugate, and Tc(I)-carbonyl chemistry enables the site-specific labeling of the histidine tag on the Affibody molecule. The goals of the present study were to prepare ^{99m}Tc-labeled His_6-$(Z_{HER2:4})_2$ and to evaluate its targeting properties compared with the targeting properties of ^{125}I-4-iodobenzoate-His_6-$(Z_{HER2:4})_2$ [^{125}I-His_6-$(Z_{HER2:4})_2$]. **Methods:** The labeling of His_6-$(Z_{HER2:4})_2$ with ^{99m}Tc was performed with an IsoLink kit. The specificity of ^{99m}Tc-His_6-$(Z_{HER2:4})_2$ binding to HER2 was evaluated in vitro with SK-OV-3 ovarian carcinoma cells. The comparative biodistributions of ^{99m}Tc-His_6-$(Z_{HER2:4})_2$ and ^{125}I-His_6-$(Z_{HER2:4})_2$ in tumor-bearing BALB/c *nu/nu* mice were determined. **Results:** The labeling yield for ^{99m}Tc-His_6-$(Z_{HER2:4})_2$ was ~60% (50°C), and the radiochemical purity was greater than 97%. The conjugate was stable during storage and under histidine and cysteine challenges and demonstrated receptor-specific binding. The biodistribution study demonstrated tumor-specific uptake levels (percentage injected activity per gram of tissue [%IA/g]) of 2.6 %IA/g for ^{99m}Tc-His_6-$(Z_{HER2:4})_2$ and 2.3 %IA/g for ^{125}I-His_6-$(Z_{HER2:4})_2$ at 4 h after injection. Both conjugates provided clear imaging of SK-OV-3 xenografts at 6 h after injection. The tumor-to-nontumor ratios were much more favorable for the radioiodinated Affibody. **Conclusion:** The use of Tc(I)-carbonyl chemistry enabled us to prepare a stable, site-specifically labeled ^{99m}Tc-His_6-$(Z_{HER2:4})_2$ conjugate that was able to bind to HER2-expressing cells in vitro and in vivo. The indirectly radioiodinated conjugate provided better tumor-to-liver ratios. The labeling of Affibody molecules with ^{99m}Tc should be investigated further.

Key Words: Affibody; HER2; Tc(I)-carbonyl chemistry; indirect iodination; tumor targeting

J Nucl Med 2006; 47:512–519

Radionuclide tumor targeting for diagnosis and therapy uses the molecular recognition of structures that ideally appear exclusively in tumor sites but, more realistically, appear at higher levels in tumors than in normal tissues. During the last decade, this methodology has been established in clinical practice; antibodies and their fragments have been used to map the expression or overexpression of tumor-related proteins, such as prostate-specific membrane antigen (*1*), carcinoembryonic antigen (*2*), TAG-72 (*3*), and Ep-CAM (*4*). The overexpression of somatostatin receptors in neuroendocrine tumors is exploited by targeting with somatostatin peptide analogs (*5*). The use of radionuclide tumor targeting for imaging enhances the possibilities of making the correct diagnosis, staging, selecting the most efficient treatment, and then monitoring the effect of therapy to guide the treatment.

One interesting target for radionuclide diagnosis is the HER2 (known also as neu, c-ErbB2, and p185) receptor, often overexpressed in carcinomas of the breast (*6*), ovary (*7*), and urinary bladder (*8*) as well as in several other carcinomas. HER2 is a transmembrane protein belonging to the human epidermal growth factor tyrosine kinase receptor family. The expression of HER2 in normal tissues is very low or not detectable (*9*). In breast cancer, the overexpression of HER2 is associated with short patient survival times (*10*) and with resistance to treatment with tamoxifen (*11*) or cyclophosphamide–methotrexate–fluorouracil therapy

Received Sep. 12, 2005; revision accepted Nov. 14, 2005.
For correspondence or reprints contact: Vladimir Tolmachev, PhD, Unit of Biomedical Radiation Sciences, Rudbeck Laboratory, 751 85 Uppsala, Sweden.
E-mail: valdimir.tolmachev@bms.uu.se

(*12*). However, breast cancers expressing HER2 respond well to anthracycline (e.g., doxorubicin)-based chemotherapy (*13*). Thus, the imaging of HER2 expression may provide clinically important information on the outcome of treatment and the progression of disease.

Recently, a new HER2-binding protein, the anti-HER2 Affibody molecule $Z_{HER2:4}$, was described (*14*). $Z_{HER2:4}$ was generated by use of phage selection of the Affibody molecule described earlier (*15*). This small, ~7-kDa, protein binds to HER2 in vitro with an affinity of about 50 nmol/L, and dimerization of $Z_{HER2:4}$ improves the affinity to 3 nmol/L (*16*). The molecular mass of the dimer $[(Z_{HER2:4})_2]$ is about 15 kDa, which is approximately half the molecular mass of single-chain antibody fragments. The small size of $(Z_{HER2:4})_2$ is an advantage for diagnosis, providing both rapid extravasation and tumor penetration and quick blood and nontarget tissue clearance. These properties are likely to provide good contrast for tumor imaging within a short time after injection.

Besides targeting properties, selection of the most suitable nuclide is important for the clinical success of a tumor-targeting conjugate. Among the radionuclides for single-photon detection, 2 nuclides, ^{123}I (half-life, 13 h) and ^{99m}Tc (half-life, 6 h), are of special interest. Their emitted γ-radiation (153 and 140 keV, respectively) is nearly ideal for imaging with γ-cameras, and their half-lives are compatible with the fast in vivo kinetics of small proteins. Previous studies demonstrated that the indirect radioiodination of $(Z_{HER2:4})_2$ with *N*-succinimidyl-4-iodobenzoate does not affect the binding of the protein to HER2 (*14,16*). Thus, in principle, ^{123}I is a possible candidate for the labeling of $(Z_{HER2:4})_2$ for imaging purposes. On the other hand, the development of a ^{99m}Tc label for $(Z_{HER2:4})_2$ is attractive because of the low price and the availability of this generator-produced nuclide (*17,18*).

The attachment of radiometals, including technetium, to peptides and proteins usually requires the attachment of a chelator (*17,19*). For synthetic peptides, the coupling of a chelator to the peptides may be integrated during synthesis and can be performed in a site-specific manner. As the complexity of the $(Z_{HER2:4})_2$ dimer makes its chemical synthesis complicated (116 amino acids), recombinant production is needed. After the biosynthesis and purification of the Affibody molecule, bifunctional chelating agents needed to bind the ^{99m}Tc have to be attached to the $(Z_{HER2:4})_2$ molecule. However, this process leads both to modification of the dimer, including lysines close to binding sites, and to random attachment of the chelator, producing a mixture of conjugates with different degrees of substitution and different positions of the label. For this reason, we chose to apply a labeling strategy with which a unique site for the attachment of technetium to the dimer is designed by means of gene engineering.

One option is the coupling of $^{99m}Tc(I)$-tricarbonyl to a histidine tag, which often is introduced into proteins to facilitate purification (*20*). Examples of the use of $^{99m}Tc(I)$-tricarbonyl $\{[^{99m}Tc(CO)_3(H_2O)_3]^+\}$ for the labeling of proteins and peptides were reviewed recently by Schibli and Schubiger (*21*). This method could be used for the site-specific labeling of the Affibody molecule because a His_6 tag was introduced originally for purification purposes into the $(Z_{HER2:4})_2$ dimer.

The main goal of this study was to evaluate the feasibility of using Affibody molecules labeled with ^{99m}Tc for the imaging of HER2 overexpression in tumors. Additional goals included establishing ^{99m}Tc labeling chemistry for $(Z_{HER2:4})_2$ by use of coupling of ^{99m}Tc to the histidine tag, evaluating the stability of the conjugate in vitro, and comparing the biodistribution of the new conjugate, ^{99m}Tc-His_6-$(Z_{HER2:4})_2$ (labeled on the histidine tag), with the biodistribution of the ^{125}I-His_6-$(Z_{HER2:4})_2$ conjugate, in which ^{125}I was used as a surrogate for the SPECT nuclide ^{123}I.

MATERIALS AND METHODS

Buffers were prepared by common methods from chemicals supplied by Merck. Construction and preparation of bivalent His_6-$(Z_{HER2:4})_2$ and its radioiodination were described earlier (*16*).

Radioactivity was measured by use of an automatic 1480 Wizard γ-counter (Wallac) equipped with an ~7.6-cm (3-in.) NaI(Tl) well detector. Instant thin-layer chromatography (ITLC) analysis was performed with ITLC silica gel plates. The distribution of radioactivity was measured with a Cyclone storage phosphor system (Packard) and analyzed with OptiQuant image analysis software (OptiQuant). Size exclusion chromatography was performed with disposable NAP-5 columns (Amersham Pharmacia Biotech AB).

Histidine Tag Labeling

A ^{99m}Tc-pertechnetate solution eluted from the generator (0.5–0.6 mL) was added to the IsoLink carbonyl labeling agent (DRN4335; Mallinckrodt), and the mixture was incubated in a boiling water bath for 20 min. The obtained solution of $[^{99m}Tc(CO)_3(H_2O)_3]^+$ (40 μL) was mixed with a solution of His_6-$(Z_{HER2:4})_2$ in phosphate-buffered saline (PBS) (40 μL, 1.2 mg/mL) and incubated at 37, 50, 70, or 100°C. At 5, 10, 20, and 40 min, samples of the crude reaction mixture were analyzed by use of ITLC and elution with PBS. The reaction mixture was purified with a NAP-5 size exclusion column. The radiochemical purity of ^{99m}Tc-His_6-$(Z_{HER2:4})_2$ was determined by use of ITLC and elution with PBS.

In Vitro Stability

In order to ensure that the technetium label in ^{99m}Tc-His_6-$(Z_{HER2:4})_2$ was stable, the conjugate was challenged with 100, 500, and 5,000 molar excesses of free L-cysteine and L-histidine (Serva) in PBS solutions for 1 h. The histidine challenge was performed at 37°C, and the cysteine challenge was performed at room temperature. In order to estimate shelf life, the conjugate was incubated at room temperature in PBS. Technetium radioactivity associated with the conjugate was evaluated after 2, 4, and 6 h of incubation by use of ITLC and elution with PBS. Validation of the method showed that free pertechnetate as well as free histidine and cysteine complexes of technetium were separated from

^{99m}Tc-His$_6$-($Z_{HER2:4}$)$_2$ and moved with the front, whereas the labeled conjugate remained at the start line.

Specificity of Binding of Labeled Conjugates to HER2-Expressing Cells

The specificity of binding of the obtained conjugates was tested with HER2-expressing SK-OV-3 ovarian cancer cells. The labeled conjugate was added to 2 groups of petri dishes (3 or 4 dishes; diameter, 3.5 cm; 2×10^5–5×10^5 cells per dish with a calculated ratio of 1 Affibody molecule of labeled conjugate per HER2 receptor). One group of dishes in each experiment was presaturated with a 1,000-fold excess of nonlabeled dimer 10 min before the labeled conjugate was added. Cells were incubated with the labeled conjugate for 1 h at 37°C, and the incubation medium was collected. Cell dishes were washed 6 times with cold serum-free medium and treated with 0.5 mL of trypsin:ethylenediaminetetraacetic acid (EDTA) solution (0.05% trypsin and 0.02% EDTA in buffer; Flow Irvin) for 10 min at 37°C. When cells were detached, 1 mL of complete medium was added to each dish, and the cells were resuspended. From the cell suspension, 1 mL was used for radioactivity measurements, and 0.5 mL was used for cell counting.

To study the influence of labeling temperature on the receptor-binding properties of ^{99m}Tc-His$_6$-($Z_{HER2:4}$)$_2$, labeling was done at 100°C, 70°C, or 50°C. Cell-binding experiments were performed with a calculated conjugate-to-receptor ratio of 1:100.

Biodistribution Studies

The animal study was approved by the local ethics committee for animal research. Female outbred BALB/c *nu/nu* mice (10–12 wk old at arrival) were acclimatized for 1 wk at the Rudbeck Laboratory animal facility before subcutaneous injection of ~5×10^6 SK-OV-3 cells into the left hind leg. Xenografts were allowed to develop for 2 mo. For anesthesia, a mixture of ketamine HCl (Ketalar; Pfizer) and xylazine HCl (Rompun; Bayer) was injected intraperitoneally.

The study protocols were the same for ^{99m}Tc-His$_6$-($Z_{HER2:4}$)$_2$ and ^{125}I-His$_6$-($Z_{HER2:4}$)$_2$. Mice were randomized into groups of 4 animals. All mice were injected subcutaneously with ~50 μL (approximately 100 kBq, 2 μg) of radiolabeled conjugate. One control group of mice was injected subcutaneously with 500 μg (200 μL) of unlabeled His$_6$-($Z_{HER2:4}$)$_2$ 45 min before radioactivity injection to block specific uptake of the radiolabeled dimer. After 1, 4, 8, and 12 h, the mice were sacrificed through heart puncture. Blood was collected with heparinized syringes (heparin, 5,000 IU/mL; Leo Pharma). Organs, tissue samples, and tumors were excised, and their radioactivity content was measured and expressed as the percentage injected activity per gram of tissue (%IA/g). The control mice, which were injected with an excess of nonlabeled dimer, were sacrificed 4 h after radioactivity injection and treated in the same way. Data calculations were performed with Prism software (GraphPad Software Inc.). The differences were considered significant if the P values from unpaired t tests were less than 0.05.

γ-Camera Imaging

The localization of both ^{99m}Tc-His$_6$-($Z_{HER2:4}$)$_2$ (8.5 MBq, 5 μg) and ^{125}I-His$_6$-($Z_{HER2:4}$)$_2$ (3 MBq, 2.3 μg) in tumors and normal organs was visualized by γ-camera imaging. Conjugates were administered by tail vein injection to BALB/c *nu/nu* mice bearing established subcutaneous SK-OV-3 tumor xenografts on their hind legs. Six hours later, animals were euthanized by an overdose of ketamine HCl and xylazine HCl. Imaging was done by use of a dual-head e.Cam γ-camera (Siemens Medical Systems, Inc.) equipped with a low-energy, high-resolution collimator. Acquisition was performed as a series of static images with a 256 × 256 matrix and a zoom factor of 3.2. The energy window settings were 35 keV, 99%, for ^{125}I and 140 keV, 15%, for ^{99m}Tc. The acquisition time was set to 10 min. Evaluation of the images was performed with a Hermes system (Nuclear Diagnostic).

RESULTS

Labeling

The coupling of $[^{99m}Tc(CO)_3(H_2O)_3]^+$ to His$_6$-($Z_{HER2:4}$)$_2$ was temperature dependent (Fig. 1). Incubation of the dimer with the carbonyl–technetium complex for 40 min provided more than a 90% yield at 70°C. This value was reduced to 61% at 50°C and 39% at 37°C. After purification with disposable NAP-5 columns, the radiochemical purity of the technetium-labeled conjugates was more that 97%.

Stability of Conjugates

The results of the stability tests are shown in Table 1. Storage in PBS for up to 6 h did not cause the release of technetium from the conjugates. The results of both cysteine and histidine challenges demonstrated high stability of the attachment of the label to the dimer. The results were comparable to previously published data for ^{99m}Tc-histidine tag–labeled compounds (*20,22*).

Specific Binding to HER2-Expressing Cells

The binding of ^{125}I-His$_6$-($Z_{HER2:4}$)$_2$ to cultured SK-OV-3 ovarian cancer cells was significantly ($P < 0.0001$) lower when a large excess of nonlabeled dimer for receptor blocking was added (data not shown), providing evidence for the receptor-mediated binding of radioactivity to HER2-expressing cells. The situation with ^{99m}Tc-His$_6$-($Z_{HER2:4}$)$_2$ was different. In vitro binding of the conjugate labeled at 50°C and 70°C was significantly ($P < 0.0001$) suppressed

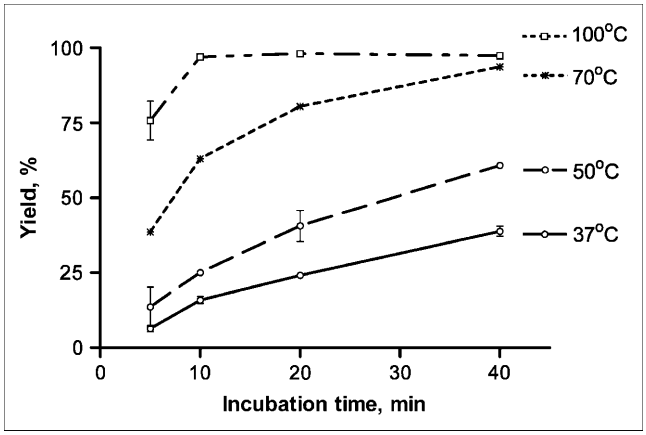

FIGURE 1. Influence of time and temperature on yield of ^{99m}Tc-His$_6$-($Z_{HER2:4}$)$_2$ obtained with IsoLink kit. $[^{99m}Tc(CO)_3(H_2O)_3]^+$ produced according to manufacturer's instructions was added to 48 μg of His$_6$-($Z_{HER2:4}$)$_2$ and incubated at 37°C, 50°C, 70°C, or 100°C. After 5, 10, 20, and 40 min of incubation, reaction mixture samples were analyzed by ITLC. Labeling yields are presented as mean from 2 independent samples ± maximum error.

TABLE 1
In Vitro Stability of ^{99m}Tc-His$_6$-($Z_{HER2:4}$)$_2$

Incubation medium	Incubation time, h	^{99m}Tc radioactivity associated with ^{99m}Tc-His$_6$-($Z_{HER2:4}$)$_2$, %*
PBS	2	99.1 ± 0.1
PBS	4	99.1 ± 0.1
PBS	6	99.0 ± 0.2
L-Cysteine (100-fold excess)	1	93.0 ± 1.0
L-Cysteine (500-fold excess)	1	88.0 ± 0.7
L-Cysteine (5,000-fold excess)	1	84.4 ± 0.3
L-Histidine (100-fold excess)	1 (37°C)	95.6 ± 0.0
L-Histidine (500-fold excess)	1 (37°C)	80.0 ± 4.0
L-Histidine (5,000-fold excess)	1 (37°C)	86.0 ± 3.0

*Each value represents mean for 2 samples ± maximum error.

by receptor blocking. For the conjugate labeled at 100°C, the cell-associated radioactivity was much lower and was not displaced by receptor saturation ($P = 0.74$), indicating that there was no specific binding in this situation. Furthermore, the capacity of ^{99m}Tc-His$_6$-($Z_{HER2:4}$)$_2$ labeled at 50°C, 70°C, and 100°C to bind to a large excess of cell-associated HER2 also was tested (Fig. 2). Cellular binding of the conjugate labeled at 50°C (mean ± SD, 35.35% ± 1.54%) was significantly higher than the binding of conjugates labeled at 70°C (3.83% ± 2.24%) ($P = 0.0003$) and at 100°C (0.59% ± 0.50%) ($P < 0.0001$).

Biodistributions in Tumor-Bearing Mice

Data on the biodistributions of the conjugates are shown in Table 2. The concentrations of radioactivity for ^{99m}Tc-His$_6$-($Z_{HER2:4}$)$_2$ and ^{125}I-His$_6$-($Z_{HER2:4}$)$_2$ in tumors were higher than the concentrations in blood already at 1 and 4 h after injection, respectively, and remained higher throughout the study. The levels of uptake of ^{99m}Tc-His$_6$-($Z_{HER2:4}$)$_2$ and ^{125}I-His$_6$-($Z_{HER2:4}$)$_2$ in tumors at 4 h after injection were significantly reduced by preinjection of a large amount of nonlabeled dimer [$P < 0.04$ for ^{99m}Tc-His$_6$-($Z_{HER2:4}$)$_2$ and $P < 0.01$ for ^{125}I-His$_6$-($Z_{HER2:4}$)$_2$]; this result is an indication of the receptor-mediated tumor uptake of these conjugates in vivo. The radioactivity retention in tumors was constant for the technetium-labeled conjugate (no significant difference between the time points), whereas the tumor-associated radioactivity for ^{125}I-His$_6$-($Z_{HER2:4}$)$_2$ constantly decreased from 3.23 ± 0.12 %IA/g at 1 h after injection to 0.68 ± 0.09 %IA/g at 12 h after injection.

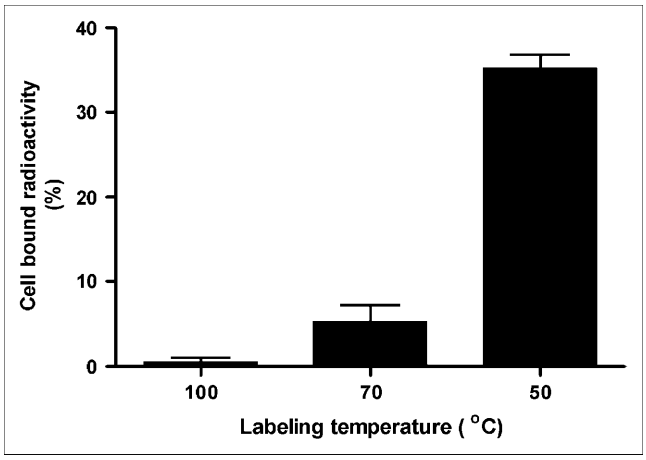

FIGURE 2. Influence of labeling temperature on binding of ^{99m}Tc-His$_6$-($Z_{HER2:4}$)$_2$ to SK-OV-3 cells. Conjugate was labeled with ^{99m}Tc by use of IsoLink kit at 100°C, 70°C, and 50°C, and cell-bound fraction was measured when conjugate was added to HER2-expressing cells at conjugate-to-antigen ratio of 1:100. Data are presented as mean for 3 dishes ± SD. Addition of 1,000-fold excess of nonlabeled His$_6$-($Z_{HER2:4}$)$_2$ reduced cellular binding to less than 1% of added radioactivity in all samples.

No significant decrease in radioactivity uptake was seen in any tissues except for tumors after the preinjection of a large amount of nonlabeled dimer. This was the case for both ^{125}I-His$_6$-($Z_{HER2:4}$)$_2$ and ^{99m}Tc-His$_6$-($Z_{HER2:4}$)$_2$ and indicates that receptor-mediated uptake plays a minor role in the distributions of these conjugates in normal organs and tissues or does not have any effect at all. Somewhat increased radioactivity uptake in some organs was seen after blocking. An altered excretion pattern after overloading with nonlabeled protein may be an explanation.

The initial clearance of both conjugates from blood was rather quick, and the concentrations in blood at 1 h after injection were 3.83 ± 0.29 %IA/g for ^{125}I-His$_6$-($Z_{HER2:4}$)$_2$ and 1.16 ± 0.16 %IA/g for ^{99m}Tc-His$_6$-($Z_{HER2:4}$)$_2$. An apparent concentration in blood at the time of injection should be 60–70 %IA/g, assuming a blood volume of 1.5 mL per mouse. The clearance rate at later times was higher for ^{125}I-His$_6$-($Z_{HER2:4}$)$_2$ than for ^{99m}Tc-His$_6$-($Z_{HER2:4}$)$_2$.

Both conjugates had high initial levels of uptake in the skin, consistent with the large interstitial volume of this tissue. However, the clearance of ^{99m}Tc-His$_6$-($Z_{HER2:4}$)$_2$ was slower than the clearance of ^{125}I-His$_6$-($Z_{HER2:4}$)$_2$. A possible reason may be a nonspecific interaction with components of the extracellular matrix of the skin.

In all tissues except for the thyroid, the iodine radioactivity decreased over time after the injection of ^{125}I-His$_6$-($Z_{HER2:4}$)$_2$. The delivery of ^{99m}Tc with ^{99m}Tc-His$_6$-($Z_{HER2:4}$)$_2$ produced the highest levels of normal organ uptake in the kidneys and the liver. The highest ^{125}I uptake levels after delivery with ^{125}I-His$_6$-($Z_{HER2:4}$)$_2$ occurred initially in the kidneys and the liver, although the levels in the liver already were decreased markedly at 4 h after injection. Apparently, better tumor–to–normal-tissue ratios for ^{125}I-His$_6$-($Z_{HER2:4}$)$_2$ were, in most cases, influenced more by the radioactivity washout from normal tissues than by the change in the accumulation of radioactivity in tumors.

γ-Camera Imaging

Images acquired at 6 h after the administration of both radioiodinated and technetium-labeled His$_6$-($Z_{HER2:4}$)$_2$ to BALB/c *nu/nu* mice bearing subcutaneous SK-OV-3 tumors

TABLE 2
Biodistributions of ^{125}I-His$_6$-($Z_{HER2:4}$)$_2$ and ^{99m}Tc-His$_6$-($Z_{HER2:4}$)$_2$ in Tumor-Bearing Mice

Organ or tissue	%IA/g of organ or tissue*											
	1 h		4 h		8 h		12 h	
	^{125}I	^{99m}Tc	^{125}I	^{99m}Tc	^{125}I	^{99m}Tc	^{125}I	^{99m}Tc
Blood	3.83 ± 0.29	1.16 ± 0.16	0.56 ± 0.14 (0.63 ± 0.09)	0.54 ± 0.04 (0.47 ± 0.14)	0.09 ± 0.03	0.54 ± 0.23	0.04 ± 0.01	0.40 ± 0.03
Heart	1.34 ± 0.12	0.70 ± 0.07	0.31 ± 0.14 (0.22 ± 0.02)	0.43 ± 0.04 (1.19 ± 0.20)	0.03 ± 0.02	0.58 ± 0.14	0.03 ± 0.01	NM
Lungs	2.56 ± 0.10	1.18 ± 0.10	0.44 ± 0.12 (0.48 ± 0.06)	0.90 ± 0.04 (1.35 ± 0.04)	0.12 ± 0.04	1.22 ± 0.12	0.06 ± 0.02	NM
Liver	5.10 ± 0.25	6.07 ± 0.42	1.00 ± 0.38 (1.06 ± 0.37)	6.97 ± 0.28 (7.38 ± 0.92)	0.09 ± 0.02	7.32 ± 3.21	0.04 ± 0.01	6.77 ± 0.53
Spleen	1.41 ± 0.10	1.27 ± 0.05	0.19 ± 0.04 (0.20 ± 0.03)	0.97 ± 0.05 (1.92 ± 0.30)	0.04 ± 0.01	1.59 ± 0.06	0.02 ± 0.01	NM
Pancreas	2.43 ± 0.08	0.79 ± 0.09	0.26 ± 0.05 (0.44 ± 0.14)	0.62 ± 0.05 (1.01 ± 0.14)	0.04 ± 0.01	1.10 ± 0.49	0.01 ± 0.01	NM
Kidneys	69 ± 10	92.53 ± 0.73	30 ± 3 (25 ± 4)	89 ± 10 (104 ± 17)	8.22 ± 2.19	79 ± 37	3.61 ± 0.86	75 ± 10
Stomach	2.26 ± 0.29	1.55 ± 0.19	0.76 ± 0.21 (0.81 ± 0.16)	1.76 ± 0.12 (1.96 ± 0.20)	0.33 ± 0.17	1.19 ± 0.38	0.05 ± 0.02	0.93 ± 0.12
Salivary glands	2.70 ± 0.53	1.63 ± 0.03	1.39 ± 0.31 (1.14 ± 0.13)	2.55 ± 0.29 (2.28 ± 0.21)	0.22 ± 0.06	1.20 ± 0.35	0.04 ± 0.02	1.20 ± 0.10
Tumor	3.23 ± 0.12	1.94 ± 0.58	2.27 ± 0.55 (0.53 ± 0.06)	2.61 ± 0.41 (1.47 ± 0.16)	1.06 ± 0.20	2.64 ± 0.86	0.68 ± 0.09	2.62 ± 0.48
Skin	3.31 ± 1.18	1.42 ± 0.19	0.27 ± 0.09 (0.80 ± 0.50)	1.69 ± 0.77 (1.94 ± 0.78)	0.12 ± 0.06	1.57 ± 0.25	0.03 ± 0.00	NM
Muscle	0.84 ± 0.12	0.34 ± 0.06	0.07 ± 0.03 (0.10 ± 0.02)	0.32 ± 0.08 (0.50 ± 0.03)	0.01 ± 0.00	0.30 ± 0.07	NM	NM
Bone	0.56 ± 0.11	0.58 ± 0.16	0.08 ± 0.04 (0.20 ± 0.09)	0.55 ± 0.18 (2.54 ± 0.99)	0.04 ± 0.01	0.81 ± 0.34	0.04 ± 0.01	NM
Thyroid	0.08 ± 0.03	0.05 ± 0.01	0.15 ± 0.07 (0.16 ± 0.02)	0.06 ± 0.01 (0.11 ± 0.01)	0.24 ± 0.08	0.03 ± 0.01	0.20 ± 0.04	0.03 ± 0.02

*Each value represents mean for 4 animals ± SD. Values for thyroid are presented as percent injected radioactivity per organ. Values in parentheses are for 4 animals that were preinjected with large molar excess of nonlabeled dimer. NM = nonmeasurable.

revealed good tumor localization and good contrast relative to the findings for the contralateral site (Fig. 3). As predicted from the results of the biodistribution studies, the renal route of elimination of the labeled conjugates also led to substantial kidney retention. Hepatic accumulation was observed at this time for both conjugates. However, the accumulation of the ^{99m}Tc label in the liver was higher than that in tumors.

DISCUSSION

The efficiency of nuclear imaging is determined by several factors, the energy of the γ-radiation emitted by the radionuclide being one of them. The γ-cameras and SPECT devices currently in use are equipped mainly with ~1-cm (3/8-in.) NaI(Tl) crystals that provide the best resolution and detection efficiency when the γ-energy is about 150 keV. Accordingly, nuclides that emit such radiation provide the best opportunity to detect small lesions for a given tracer and a given dose burden to patients. Among the nuclides that are commercially available for γ-scintigraphy, ^{99m}Tc and ^{123}I have the best nuclear properties. Radioiodination of the anti-HER2 Affibody was reported earlier (*14*), and it was demonstrated that the use of an indirect labeling method with *N*-succinimidyl-4-iodobenzoate provided a conjugate with good targeting properties (*16*). However, the use of ^{99m}Tc would render the labeled conjugate less expensive and more readily available at clinics.

In the present study, we used a His_6 tag as a binding site for ^{99m}Tc. This approach provided a well-defined position for the label, which is situated at some distance from the binding region of the Affibody molecule. As our previous experience showed that modification of lysines, which are commonly used for the coupling of bifunctional chelators, might affect the binding of the conjugate to HER2, site-specific labeling was preferable. In addition, the use of a His_6 tag simplified the production and characterization of the targeting molecule. The His_6 tag acts in this case as a bifunctional chelator and may affect the biodistribution of a recombinant protein. Although Waibel et al. (20) did not observe a negative effect of a ^{99m}Tc(I)-tricarbonyl-His_6 label on the biodistribution of a single-chain variable fragment of antibody in comparison with the effect of radioiodination, some studies reported higher levels of uptake of radioactivity by the liver than would be expected for the studied proteins (*23,24*). An increase in lipophilicity attributable to ^{99m}Tc(I)-tricarbonyl was identified as one of the problems associated with this method (*25*).

An attachment of an atom or group of atoms during labeling may modify the biokinetics of a peptide or a small protein because of structural changes or modification of charge or lipophilicity (*26–29*). Moreover, it has been observed that, for technetium, amino acids in proximity to a chelator may influence complex formation. As a result, the same chelator may provide different stabilities of technetium attachment in different proteins, and it is difficult to predict

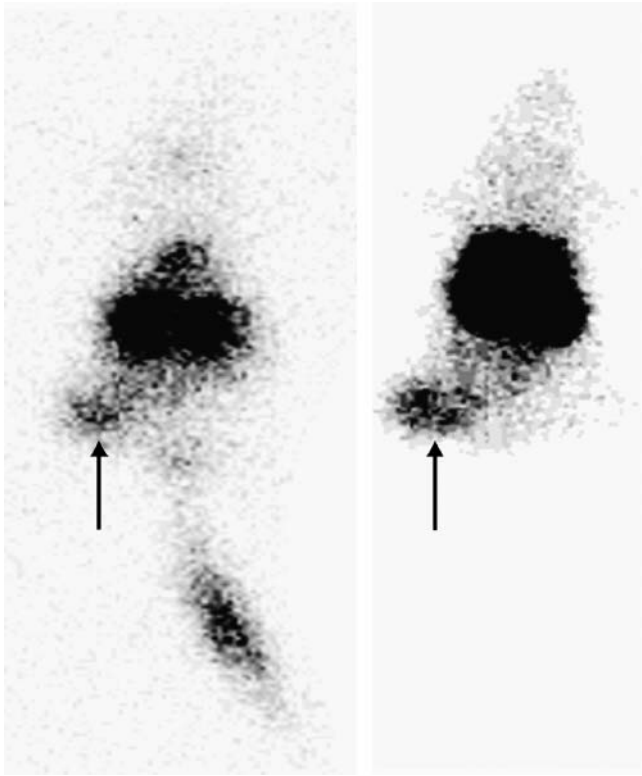

FIGURE 3. Anterior whole-body images of representative BALB/c *nu/nu* mice with subcutaneous HER2-expressing SK-OV-3 human breast cancer xenografts. Images were obtained 6 h after injection of ^{125}I-His$_6$-$(Z_{HER2:4})_2$ (left) and ^{99m}Tc-His$_6$-$(Z_{HER2:4})_2$ (right). Tumors (arrows) can be seen clearly.

the stability of labeling and the pharmacokinetics of technetium-labeled substances. It was previously emphasized that it is important to compare chelators and labeling methods before selecting a ^{99m}Tc labeling method for any particular peptide (*30*). The situation with radioiodination is simpler, as iodine forms a stable covalent bond with the carbon of tyrosine or with the pendant group attached to lysine and most likely would not be removed from the protein unless the protein were enzymatically degraded. Tumor retention of radioiodine may be poor in the case of internalizing targeting proteins because lipophilic radiocatabolites "leak" from tumor cells (*31*).

The in vitro binding of both conjugates to HER2-expressing SK-OV-3 cells was receptor specific. However, it was important not to exceed 50°C during the labeling of His$_6$-$(Z_{HER2:4})_2$ with ^{99m}Tc by use of the IsoLink kit, because a high labeling temperature reduced the receptor-binding capacity. Labeling at 50°C provided good yields, and after simple purification with disposable size exclusion columns, the radiochemical purity of the product should be sufficient for clinical applications. The in vitro stability of the technetium label was satisfactory, and the in vivo studies confirmed good stability of the label.

The ^{99m}Tc-His$_6$-$(Z_{HER2:4})_2$ conjugate targeted tumors in vivo. Because the uptake of the conjugate in tumors could be blocked significantly by preinjection of a nonlabeled conjugate, it was clear that the uptake was receptor mediated. At the same time, preinjection of a nonlabeled conjugate did not decrease the radioactivity uptake in any other organ or tissue; this result indicates that the uptake was receptor specific only in tumors. The level of tumor uptake was about 2.5 %IA/g, a value that is comparable to the tumor uptake of, for example, ^{111}In-OctreoScan (*32*), which can be considered a gold standard in tumor targeting. There was no decrease in technetium radioactivity in tumors up to at least 12 h; this result is an indication of good residualizing properties of this technetium label in vivo. This conclusion is supported further by the fact that the technetium uptake in excretory organs, such as the liver and kidneys, in which the conjugate also should be internalized, did not show an appreciable decrease as a function of time. Good in vivo stability of the label was confirmed by the low radioactivity concentrations in blood, the stomach, and the salivary glands. The level of thyroid uptake was low in comparison with that obtained with the radioiodinated conjugate.

The tumor-to-blood ratio for ^{99m}Tc-His$_6$-$(Z_{HER2:4})_2$ was about 5 at 4 h after injection and increased throughout the study. At that time point, the radioactivity concentration in tumors exceeded the concentration in a majority of tissues and organs by severalfold and increased over time. There were, however, exceptions: the spleen had an interesting uptake pattern characterized by a significant decrease in uptake from 1 h to 4 h ($P = 0.0025$) but by increased uptake from 4 h to 8 h ($P = 0.0004$). Given that the concentration of the radioactivity in blood was lower than that in the spleen at all time points, these findings may be explained by the redistribution of radiocatabolites. Renal uptake was high, as is typical for peptides and small proteins, which can pass through the glomerular membrane (*33*). Although this property may present a problem for the imaging of targets located close to the kidneys, it does not preclude the clinical use of radiolabeled short peptides or small proteins for imaging purposes. Primary breast carcinomas, which are considered to be the first candidates for the imaging of HER2 expression, are well separated anatomically from the kidneys and are not obscured by kidney radioactivity accumulation. However, the level of uptake in the liver was higher than the level of uptake in tumors throughout the study. Apparently, it was not receptor specific, because it was not decreased by the preinjection of a large amount of nonlabeled protein. The liver uptake also may have been attributable to the somewhat higher lipophilicity of the technetium-labeled conjugate than of the radioiodinated construct. In general, a higher lipophilicity of radiolabeled peptides is associated with hepatobiliary excretion (*26,28,34*). Preliminary studies with the Affibody molecule labeled with ^{111}In by use of a hydrophilic benzyl-diethylenetriamine-pentaacetic acid chelator have shown a level of liver uptake significantly lower than that obtained with ^{99m}Tc-His$_6$-$(Z_{HER2:4})_2$ (*35*). The fact that the liver often is the site of formation of metastases could be an obstacle for the introduction of this conjugate into clinical practice, limiting its use

to the imaging of HER2 only in extrahepatic metastases. Still, the good imaging properties, low price, and availability of ^{99m}Tc render it an attractive label and suggest that further investigations of the technetium labeling of Affibody molecules are warranted.

Two major gene engineering approaches are considered. The first is increasing the overall hydrophilicity of the ^{99m}Tc-labeled Affibody molecule by polar or negatively charged amino acids outside the binding site. The second approach includes the introduction of peptide sequences at one of the termini, which would provide N_4 or N_3S donors for the Tc=O core. An attractive aspect of this approach is the possibility of manipulating the charge and polarity of the chelating sequence by changing the side chains of the amino acids (*28*).

Data on the biodistribution of ^{125}I-His$_6$-$(Z_{HER2:4})_2$ indicate that the radioiodine label may be a better label than technetium for the imaging of HER2 expression in tumors. At 1 and 4 h after injection, the levels of tumor uptake of the radioiodinated conjugate were as high as the levels of uptake of the technetium-labeled protein. The initial level of liver uptake also was relatively high when the radioiodinated conjugate was used, but it already had decreased at 4 h. The tumor uptake was receptor mediated and, as with technetium, blocking was efficient only in tumors and not in normal organs and tissues. The major difference in tumor uptake between ^{125}I-His$_6$-$(Z_{HER2:4})_2$ and ^{99m}Tc-His$_6$-$(Z_{HER2:4})_2$ was that radioiodine levels decreased over time. However, the decrease in the accumulation in tumors was slower than that in normal organs, and the tumor–to–normal-organ ratios increased over time. Most importantly, the levels of accumulation in tumors were higher than those in the liver. At 8 h after injection, the radioactivity concentration in tumors was 16.1 ± 3.4 times higher than that in the liver; this result should enable the imaging of HER2 expression in liver metastases. The possibility of visualizing HER2 expression in liver metastases is a major advantage of the radioiodinated conjugate.

CONCLUSION

The use of histidine tag labeling enabled us to create stable site-specific technetium labeling of a specific anti-HER2 Affibody dimer. The use of ^{99m}Tc-His$_6$-$(Z_{HER2:4})_2$ enabled the imaging of HER2-expressing xenografts in mice. This conjugate may be useful for the imaging of HER2 expression in primary breast carcinomas and their extrahepatic metastases. The liver uptake levels for ^{99m}Tc-His$_6$-$(Z_{HER2:4})_2$, however, were higher than those for ^{125}I-His$_6$-$(Z_{HER2:4})_2$, which had somewhat lower levels of tumor uptake but a better tumor-to-liver ratio.

ACKNOWLEDGMENTS

Financial support for this study was partially provided by the Swedish Cancer Society and partially by Affibody AB.

REFERENCES

1. Polascik TJ, Manyak MJ, Haseman MK, et al. Comparison of clinical staging algorithms and ^{111}indium-capromab pendetide immunoscintigraphy in the prediction of lymph node involvement in high risk prostate carcinoma patients. *Cancer.* 1999;85:1586–1592.
2. Hughes K, Pinsky CM, Petrelli NJ, et al. Use of carcinoembryonic antigen radioimmunodetection and computed tomography for predicting the resectability of recurrent colorectal cancer. *Ann Surg.* 1997;226:621–631.
3. Muxi A, Pons F, Vidal-Sicart S, et al. Radioimmunoguided surgery of colorectal carcinoma with an ^{111}In-labelled anti-TAG72 monoclonal antibody. *Nucl Med Commun.* 1999;20:123–130.
4. Breitz HB, Tyler A, Bjorn MJ, et al. Clinical experience with Tc-99m nofetumomab merpentan (Verluma) radioimmunoscintigraphy. *Clin Nucl Med.* 1997;22:615–620.
5. Behr TM, Behe M, Becker W. Diagnostic applications of radiolabeled peptides in nuclear endocrinology. *Q J Nucl Med.* 1999;43:268–280.
6. Carlsson J, Nordgren H, Sjostrom J, et al. HER2 expression in breast cancer primary tumours and corresponding metastases: original data and literature review. *Br J Cancer.* 2004;90:2344–2348.
7. Meden H, Kuhn W. Overexpression of the oncogene c-erbB-2 (HER2/neu) in ovarian cancer: a new prognostic factor. *Eur J Obstet Gynecol Reprod Biol.* 1997;71:173–179.
8. Wester K, Sjostrom A, de la Torre M, et al. HER-2: a possible target for therapy of metastatic urinary bladder carcinoma. *Acta Oncol.* 2002;41:282–288.
9. Natali PG, Nicotra MR, Bigotti A, et al. Expression of the p185 encoded by HER2 oncogene in normal and transformed human tissues. *Int J Cancer.* 1990; 45:457–461.
10. Gancberg D, Di Leo A, Cardoso F, et al. Comparison of HER-2 status between primary breast cancer and corresponding distant metastatic sites. *Ann Oncol.* 2002;13:1036–1043.
11. Carlomagno C, Perrone F, Gallo C, et al. c-erb B2 overexpression decreases the benefit of adjuvant tamoxifen in early-stage breast cancer without axillary lymph node metastases. *J Clin Oncol.* 1996;14:2702–2708.
12. Gusterson BA, Gelber RD, Goldhirsch A, et al. Prognostic importance of c-erbB-2 expression in breast cancer. International (Ludwig) Breast Cancer Study Group. *J Clin Oncol.* 1992;10:1049–1056.
13. Muss HB, Thor AD, Berry DA, et al. c-erbB-2 expression and response to adjuvant therapy in women with node-positive early breast cancer. *N Engl J Med.* 1994;330:1260–1266.
14. Wikman M, Steffen AC, Gunnieriusson E, et al. Selection and characterisation of HER2/neu-binding Affibody ligands. *Protein Eng Des Sel.* 2004;17:455–462.
15. Nord K, Gunneriusson E, Ringdahl J, et al. Binding proteins selected from combinatorial libraries of an alpha-helical bacterial receptor domain. *Nat Biotechnol.* 1997;15:772–777.
16. Steffen AC, Wikman M, Tolmachev V, et al. *In vitro* characterization of a bivalent anti-HER-2 Affibody with potential for radionuclide-based diagnostics. *Cancer Biother Radiopharm.* 2005;20:239–248.
17. Liu S, Edwards DS, Barrett JA. ^{99m}Tc labeling of highly potent small peptides. *Bioconjug Chem.* 1997;8:621–636.
18. Jurisson SS, Lydon D. Potential technetium small molecule radiopharmaceuticals. *Chem Rev.* 1999;99:2205–2218.
19. Liu S, Edwards DS. ^{99m}Tc-Labeled small peptides as diagnostic radiopharmaceuticals. *Chem Rev.* 1999;99:2235–2268.
20. Waibel R, Alberto R, Willuda J, et al. Stable one-step technetium-99m labeling of His-tagged recombinant proteins with a novel Tc(I)-carbonyl complex. *Nat Biotechnol.* 1999;17:897–901.
21. Schibli R, Schubiger PA. Current use and future potential of organometallic radiopharmaceuticals. *Eur J Nucl Med Mol Imaging.* 2002;29:1529–1542.
22. Du J, Hiltunena J, Marquez M, et al. Technetium-99m labelling of glycosylated somatostatin-14. *Appl Radiat Isot.* 2001;55:181–187.
23. Francis RJ, Mather SJ, Chester K, et al. Radiolabelling of glycosylated MFE-23::CPG2 fusion protein (MFECP1) with ^{99m}Tc for quantitation of tumour antibody-enzyme localisation in antibody-directed enzyme pro-drug therapy (ADEPT). *Eur J Nucl Med Mol Imaging.* 2004;31:1090–1096.
24. Pimentel GJ, Vazquez JE, Quesada W, et al. Hexa-histidine tag as a novel alternative for one-step direct labelling of a single-chain Fv antibody fragment with ^{99m}Tc. *Nucl Med Commun.* 2001;22:1089–1094.
25. Ballinger JR, Cooper MS, Mather SJ. Re: controversies—$[Tc(CO)_3]^+$ chemistry: a promising new concept for SPET? *Eur J Nucl Med Mol Imaging.* 2004;31: 304–305.
26. Verbeke K, Snauwaert K, Cleynhens B, et al. Influence of the bifunctional chelate on the biological behavior of ^{99m}Tc-labeled chemotactic peptide conjugates. *Nucl Med Biol.* 2000;27:769–779.

27. Rusckowski M, Qu T, Gupta S, et al. A comparison in monkeys of ^{99m}Tc labeled to a peptide by 4 methods. *J Nucl Med.* 2001;42:1870–1877.
28. Decristoforo C, Mather SJ. The influence of chelator on the pharmacokinetics of ^{99m}Tc-labelled peptides. *Q J Nucl Med.* 2002;46:195–205.
29. Tolmachev V, Orlova A, Wei Q, et al. Comparative biodistribution of potential anti-glioblastoma conjugates [^{111}In]DTPA-hEGF and [^{111}In]Bz-DTPA-hEGF in normal mice. *Cancer Biother Radiopharm.* 2004;19:491–501.
30. Qu T, Wang Y, Zhu Z, et al. Different chelators and different peptides together influence the *in vitro* and mouse *in vivo* properties of ^{99m}Tc. *Nucl Med Commun.* 2001;22:203–215.
31. Tolmachev V, Orlova A, Lundqvist H. Approaches to improvement of cellular retention of radiohalogen labels delivered by internalizing tumor targeting proteins and peptides. *Curr Med Chem.* 2003;10:2447–2460.
32. Froidevaux S, Heppeler A, Eberle AN, et al. Preclinical comparison in AR4-2J tumor-bearing mice of four radiolabeled 1,4,7,10-tetraazacyclododecane-1,4,7,10-tetraacetic acid-somatostatin analogs for tumor diagnosis and internal radiotherapy. *Endocrinology.* 2000;141:3304–3312.
33. Behr TM, Goldenberg DM, Becker W. Reducing the renal uptake of radiolabeled antibody fragments and peptides for diagnosis and therapy: present status, future prospects and limitations. *Eur J Nucl Med.* 1998;25:201–212.
34. Decristoforo C, Mather SJ. Technetium-99m somatostatin analogues: effect of labelling methods and peptide sequence. *Eur J Nucl Med.* 1999;26: 869–876.
35. Orlova A, Nilsson F, Magnusson M, et al. ^{111}In-Bz-DTPA-$Z_{HER2:342}$, a candidate for imaging of HER2-expression in malignant tumors [abstract]. *J Labelled Comp Radiopharm.* 2005;48(suppl):S51.

JNM The Journal of NUCLEAR MEDICINE

Comparative In Vivo Evaluation of Technetium and Iodine Labels on an Anti-HER2 Affibody for Single-Photon Imaging of HER2 Expression in Tumors

Anna Orlova, Fredrik Y. Nilsson, Maria Wikman, Charles Widström, Stefan Ståhl, Jörgen Carlsson and Vladimir Tolmachev

J Nucl Med. 2006;47:512-519.

The Journal of Nuclear Medicine is published monthly.
SNMMI | Society of Nuclear Medicine and Molecular Imaging
1850 Samuel Morse Drive, Reston, VA 20190.
(Print ISSN: 0161-5505, Online ISSN: 2159-662X)

SNMMI SOCIETY OF NUCLEAR MEDICINE AND MOLECULAR IMAGING